Segmentation and measurement of lung pathological changes for COVID-19 diagnosis based on computed tomography

Yousif A. Hamad [1,2*], Mohammed E. Seno [3], Mohannad Al-Kubaisi [3], Anastasiia N. Safonova [1, 4]

[1] Deep Learning Laboratory, Siberian Federal University, Krasnoyarsk, Russian Federation,
[2] Collage of information technology, Imam Ja'afar Al-sadiq University, Kirkuk, Iraq
[3] Department of Computer Science, Al-Maarif University College, Ramadi, Iraq,
[4] Department of Computer Science and Artificial Intelligence, University of Granada, 18071 Granada, Spain

ABSTRACT

Coronavirus 2019 (COVID-19) spread internationally in early 2020, resulting from an existential health disaster. Automatic detecting of pulmonary infections based on computed tomography (CT) images has a huge potential for enhancing the traditional healthcare strategy for treating COVID-19. CT imaging is essential for diagnosis, the process of assessment, and the staging of COVID-19 infection. The detection in association with computed tomography faces many problems, including the high variability, and low density between the infection and normal tissues. Processing is used to solve a variety of diagnostic tasks, including highlighting and contrasting things of interest while taking color-coding into account. In addition, an evaluation is carried out using the relevant criteria for determining the alterations nature and improving a visibility of pathological changes and an accuracy of the X-ray diagnostic report. It is proposed that pre-processing methods for a series of dynamic images be used for these objectives. The lungs are segmented and parts of probable disease are identified using the wavelet transform and the Otsu threshold value. Delta maps and maps created with the Shearlet transform that have contrasting color coding are used to visualize and select features (markers). The efficiency of the suggested combination of approaches for investigating the variability of the internal geometric features (markers) of the object of interest in the photographs is demonstrated by analyzing the experimental and clinical material done in the work. The suggested system indicated that the total average coefficient obtained 97.64% regarding automatic and manual infection sectors, while the Jaccard similarity coefficient achieved 96.73% related to the segmentation of tumor and region infected by COVID-19.

Keywords:	Computed Tomography, Wavelet Transform, Image Segmentation, Contours Detection, COVID-19.

Corresponding Author:

Yousif A. Hamad
Deep Learning Laboratory, Siberian Federal University, Krasnoyarsk, Russian Federation
Collage of information technology, Imam Ja'afar Al-sadiq University, Kirkuk, Iraq
E-mail: y.albayati8@gmail.com

1. Introduction

It is very important to discover the disease in the patient as early as possible, especially in the detection of the infected regions of CT before leading to malignant tumors. Medical image processing plays an essential part in diagnosing many diseases and contour detection. It is shown that the developed automated diagnosis software allows improving the image quality of the segmented objects (infected regions or tumors) under study and increasing the amount of information stored in the database, as well as solving the problems of approximation and visualization of data with improved accuracy. The malignant tumors and COVID-19 in chest CT is a public problem of health. Estimates of the prevalence of lung cancer over 5 years in 2012 exceeded 825,000 cases, which is the third common type of cancer after breast[1, 2]. And Up to 29 April 2020, more than 3 million cases of COVID-19 have been stated in over 200 nations , causing around 230,690 deaths [3]. Besides, there is no effectual treatment at this moment in time[4]. Based on the national chest screening test, a low-dose tomography examination can decrease the lung cancer death rate by 25% compared to chest x-ray images[5]. Early diagnosis is important to foreboding and has a major impact on planning treatment [6-8]. The automatic detection of lung boundaries and infected regions (COVID-19) is important to step of CT scans and analysis. It is an instrument of early indicative typically utilized in clinical projects to control heart absconds, including lung illness, heart, dying, mass, chest, pleural radiation, broadened heart, and expansion [9, 10]. Concerning the presence of sporadic lung shape, the size of the left and right aspect of the lung, the absolute volume of the lung [11, 12]

means that genuine sicknesses, for example, a developed heart, COVID-19, or hidden tumors in the lung and the event of an appearance leading to cancer. The danger of this disease lies in hidden tumors [13, 14]. Automating the diagnosis and analysis of CT medical images has always been one of the most interesting areas of developing a computer-aided diagnosis system. The definition and segmentation of the tumors for CT images of the Society Associated to Fleischer's is "a round opacity, at least moderately well margined and no greater than 3 cm in maximum diameter" [15]. The segmentation of nodules on CT images indicates the dividing of a digital image into several areas or groups of pixels[16-18]. Effective and efficient diagnostic systems using computer-aided diagnostics (CAD) are highly desirable [16, 19, 20]. Since these systems are regularly designed to offer a doctor with a 2nd opinion [15] to concentrate consideration on doubtful areas of the image, the game Role "The second reader." A typical CAD system architecture includes image pre-processing, identifying a region (COVID-19) of interest, extracting and selecting characteristics, and classification. Over the previous years, a few scientists proposed different strategies for CT picture division, which permits acquiring lung limits [21-24]. These techniques utilize various methodologies. In this way, very well may be used a standard-based methodology, which contains groupings of steps and rules, for example, the thresholding or morphological activities. Strategies dependent on this methodology have generally direction suppositions and register rough arrangements. Results can utilize for tuning ventures for more powerful hashing (division) calculations [17]. The techniques of processing images are employed on chest radiographs to specify areas of the lung, their size measurements, and shape irregularities, the images on the chest CT in the evaluation of clinical is important to identify lung disease [10, 25]. A new network for the deep screening of pulmonary infection COVID-19 (Inf-Net) was suggested for the automatic identification of affected areas of CT of the chest [26]. Lately, numerous papers have been provided and obtained performances of the infection region of COVID-19. These algorithms used an automated segmentation of the lung and infection region of COVID-19 on CT images. For example, [26, 11] utilized the Deep Network (Inf-Net) t to automatically recognise infected regions of COVID-19 from chest CT scans. Oulefki et al. [27] presented an automated COVID-19 lung infected region segmentation to improve the performance. The paper presents the following: a way of interpreting pathological alterations in the lungs on CT scans with COVID-19, incorporating models and texture analysis approaches. The strategy aims to increase the visibility of these regions to increase diagnosis accuracy and broaden the radiological conclusion. On low-dose CT scans, it is projected to investigate the textural feature based on "frosted glass" manifestation. This allows you to limit the patient's radiation dose without sacrificing image quality.

2. Methods and materials

The main stages include preliminary processing, segmentation (entire lung, nodules, and infected regions of COVID-19), and the formation of an outline exemplification with color-coding, feature extraction, and data analysis. Recoverable signs will shift contingent upon the reason for the clinical investigation. The proposed treatment is presented in Figure 1.
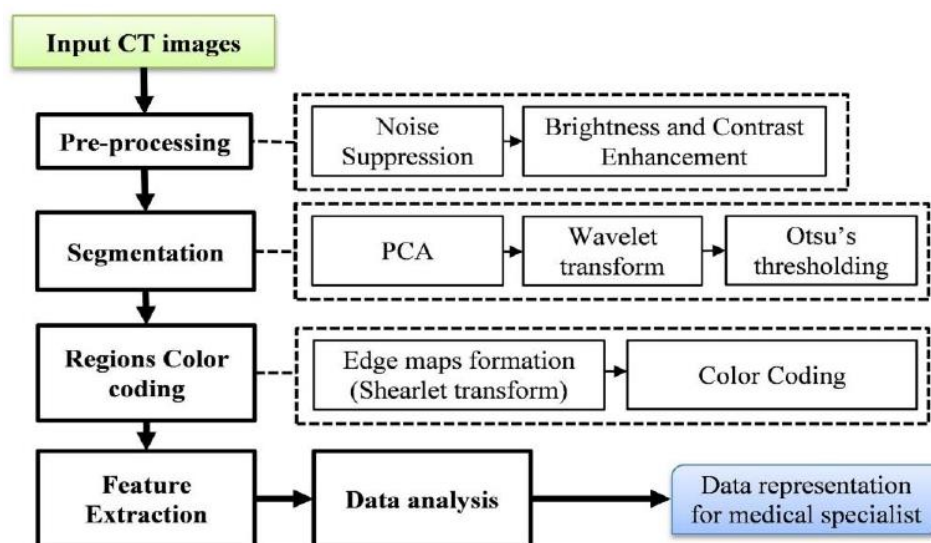

Figure 1. The structural scheme of the suggested method for CT images analysis

2.1. CT images pre-processing

The foremost task of pre-processing is improving a quality of CT images [28-31]. This stage can develop CT image characters (for example, noise reduction) and enhance the appearance through deleting unwanted parts from the background. Since the CT image is denoted as a group of individual pixels, used to perform separate factions of the Gauss function earlier of applying the deformation convolution. Based on the size of the kernel and σ, some parameters may go beyond the scope of the core. Thus, the size of the kernel can be cut off at this located place. In some cases, the size of the kernel is further truncated. A descriptive view is combined on the basis of many criteria especially when pathological changes are available:

- The pathological changes related to ratio and localization to supplementary configurations of the lung.
- Arithmetic constituent of the changes identified.
- Defining the formula of pathological formation and contours.
- Measuring the mass changes which are pathological in three planes (once performing multi-detector computed tomographic (MDCT)).
- The changes in intensity characterize the density of tissue owing to prevailing several constituents in its structure.
- In controversial cases, the existence of a component that is vascular or necrosis in the tissues.

Those standards have been considered as the foundation intended for analyzing images not just illustrating pathological changes, but they are also considered as communication was amongst a radiologist and physicians of other specialties. By depending on the aforementioned standards, image processing is available. A typical RS processing image is indicated in Figure 2.
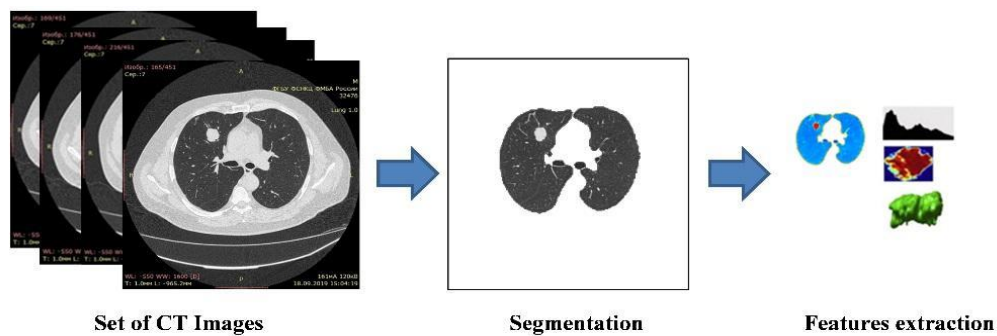

Set of CT Images   **Segmentation**   **Features extraction**

Figure 2. Stages of medical image processing

As CT images include various brightness features and contrasting ones it had been unequivocal to make use of the Multi-Scale Retinex (MSR) modification where a transforming wavelet was employed for speeding up the calculations [29] to make an accurate brightness and a contrast which is local in the interest area. Calculating texture features is allowed by a brighter depiction in the lung and assessing the lesion's structural properties. Once the features calculations, the info related to performed correction is carried out by MSR in the shape of color-coded delta maps are employed too. Maps of formed delta offer a chance to perform an introductory assessment for remains in the interest area. A case of processing CT images is indicated in Figure 3. For showing crystal clarity, during the formation of delta maps, multipliers were used, therefore, for the delta map of brightness was used multiplier 5 and for edge delta map 10.
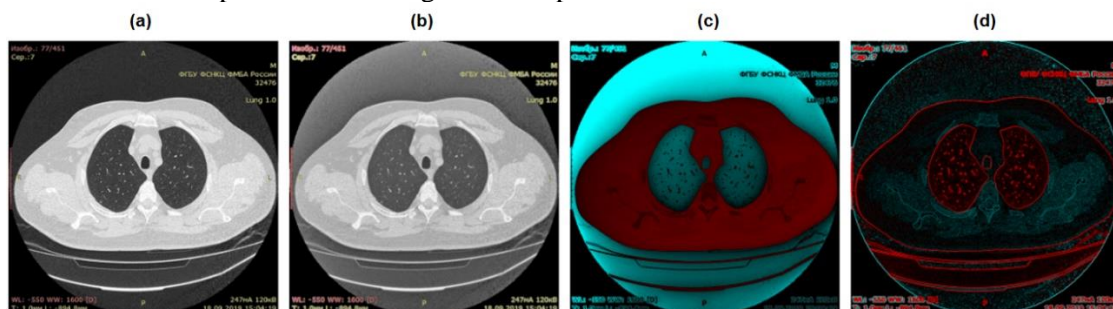

(a)   (b)   (c)   (d)

Figure 3. Processing image: (a) an original image, (b) a form of image afterward suppressing noise and MSR

processing, (c) brightness delta map, and (d) edge delta map

CT images, based on the taking image conditions, include various brightness indicators and contrast, thus, to enhance the contrast of the images, it is suggested to employ the modified method of MSR, modification in the herpes simplex virus (HSV) color space, whereof the discrete wavelet transform was employed to accelerate the computations.

2.2 Segmentation

The threshold is an important technology in applications of medical image CT segmentation. The main idea of the threshold is to specify the minimum gray level of separating region of interest (ROI) in an image from the background according to the distribution of the gray level. While people can easily distinguish the object from a complex background, the image threshold value is a challenging task to get from the image, because the accuracy of segmentation depends upon the threshold value[32-34]. After the images have been pre-processed, these are converted into grayscale images using Principal Component Analysis (PCA). Often, important image functions visually disappear when converting colour photographs to shades of gray. The PCA reduces these losses by trying to preserve the characteristic features of the colour image and convert it to a grayscale image. Converting a colour photo to shades of gray - a decreasing problem. The PCA helps to calculate the elliptical constraint in the colour space and is the least suitable square of dots that represent all colour values of the image. Then, the converted grayscale images are used in morphological processing. These operators are particularly useful for common usage to include noise removal and image enhancement. Morphological closure is performed to the image in grayscale to rise the boundaries of the front regions and get rid of tiny holes found in the CT image using a shaped appropriate structural diameter. Figure 4 shows the performance of morphological closure.
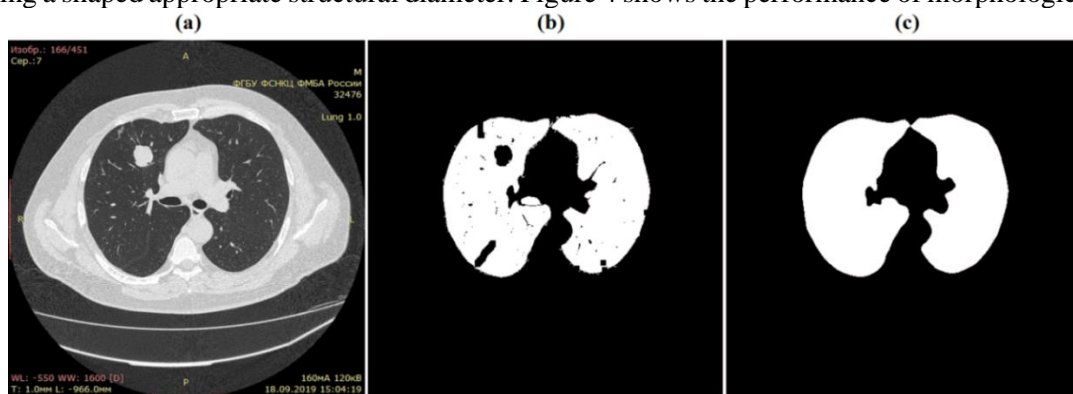

Figure 4. Results of applying morphological closure of segmented lung, (a) original image, (b) before morphological closure, and (c) after morphological closure

The next step is to find the thresholds from the morphological images using the discrete wavelet transform (DWT). It is a fundamental tool of signals and medical image processing, as removing noise and segmentation, which according to the DWT can get the automatic threshold value. In this system, Level-1 2-D wavelet decomposition is carried out to the subsequent image and look for the onsets[35-37], which can reduce the intensity of the contrast within the layer (contrast within doubled classes, regions that are black and white) in every single constituent of the image decomposed. Then calculating the new-onset (gray-level) from the sum of the four Otsu onsets and dividing by 2. Then restore the image through the DWT application and quantizing the restored image with the calculated Otsu threshold to decrease the grayscale information amount and converting it to the binary image that is (black and white). As a result, local objects of interest are picked and contrasted using texture (geometric) analysis models, based on color-coding. The study's main focus of [29]is on analyzing the texture (homogeneity and entropy) of the zone of pathological changes, as well as the intensity level regulation and adaptability in histogram analysis. Methods of segmentation can be used to solve a variety of difficulties in the examination of pathological alterations. In the figure below (Figure 5), the afflicted areas were segmented in an existence of infected parenchyma in each lung.
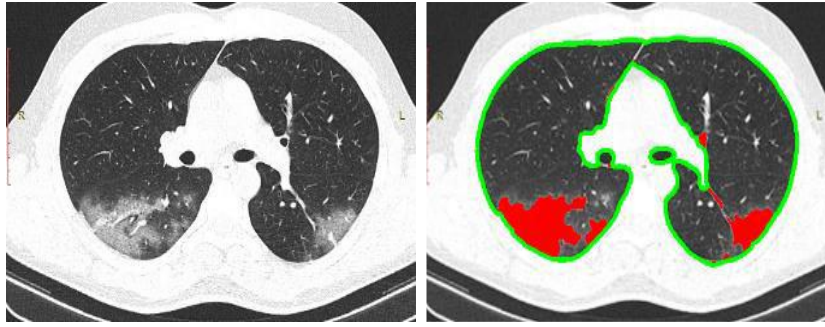
Figure 5. Segmentation of areas of the parenchyma involved

The zones associated with COVID-19 have been underlined as the majority of representative image in the series above the provided photos, with zones of red and purple colors in comparison to the blue or green color of the unaffected pulmonary parenchyma. The moment of the ratio of soft tissues and cellulose, which is as well of distinct hues and is connected with the varying densities of these structures, is equally intriguing. In this method, the process of calculating the gray-level (threshold) value of each pixel is carried out from the average value of estimated and detailed constituents of the wavelet transform. Consequently, the binary outcomes are significantly developed to the empirical outcomes, particularly for those images having hairlines and colour plates. To decide a framework of the lung's limits, the CT images are expectedly separated into equal parts. An arched structure is worked for the two parts to give a lot of focuses to the plane[38-41]. From that point forward, the two parts are consolidated in one image. Lastly, a contour representation is formed by the Shearlet transform. Considering the upshots of segmenting and representing formed maps relied on the color-coding the calculation of texture attributes urgent to attain an estimate is performed (the size of the left and right lung and tumour in the CT image, boundaries of the lung, nodules, infected regions and the funniest blood flow to the tumour). Obtained segmented CT images are useful in medical diagnostics by medical professionals. Consequently, information about lung segmentation allows us to estimate the size and characteristics of the lungs, which is useful for medical evaluation.

2.3 Database

Datasets for CT images used to evaluate the effectiveness of the developed algorithm have been tested by the CT images (tumors and nodules) datasets of General Hospital in Krasnoyarsk / Russia and for infected regions of disease (COVID-19) from [24, 25]. The data set format is DICOM, and it contains 120 CT scans of size 512 x 512, including different nodules in size and location on the lung.

2.4 System performance

The effectiveness of the contours and nodules detection of the lung was measured based on the following measures: The Pratt Figure Measurement (PFM) represents the similarity between the two contours level and is determined as follows:

$$PFM = \frac{1}{\max(RE_{Cnt}, AE_{Cnt})} \cdot \sum_{i=1}^{AE_{Cnt}} \frac{1}{1 + \alpha \cdot d_i^2}$$

(1)

Sensitivity (also known as the true positive rate, the recall): It attempts to measure the proportion of the actual positive that is identified correctly:

$$Sensivity = \frac{TP}{TP + FN}$$

(2)

The coefficient of Jaccard similarity index signifies overlapping metrics is defined as:

$$\Omega = \frac{TP}{TP + FP + FN}$$

(3)

The other measure of overlapping is the coefficient of Dice Similarity Coefficient (DSC), defined as:

$$DSC = \frac{2 \cdot TP}{2 \cdot TP + FP + FN}$$

(4)

3. Experiments and results

The findings of calculations were achieved in the tentative section of the paper utilizing a computed tomography database to assess lung diseases related to COVID-19 (Handbook of COVID-19 Prevention and Treatment, 2020). Based on 2D sections (patterns) of computed tomography of the lungs, a series of computations were performed to depict the damaged regions. The computational approach for assessing the degree of lung injury allows for more precise determination of the pathology zone's borders. As a result, the accuracy of the area estimate and the severity assessment of condition improves.

To evaluate the effectiveness of the developed methods, the contour of the CT image of lungs was determined and nodules, infected regions were detected in different image databases described in the following sections. Visual representations of detected lung boundaries and nodules are presented in Figure 6.
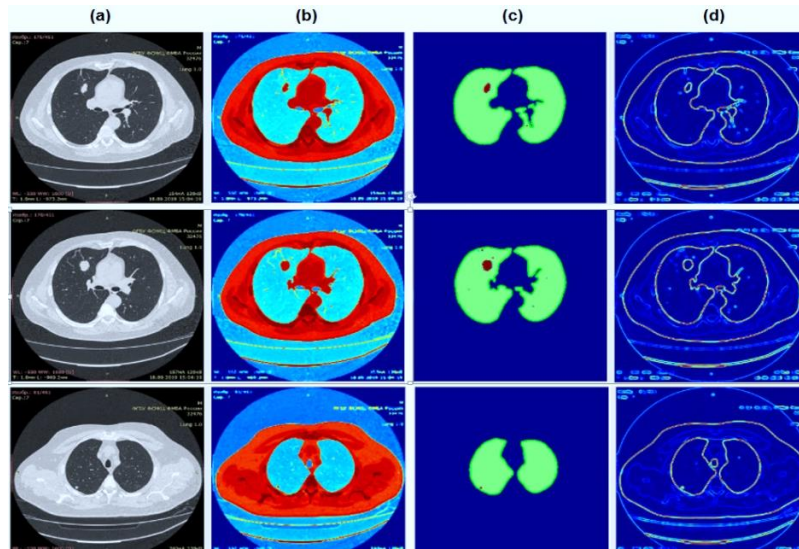

Figure 6. Lung regions in CT images with different nodules, (a) original CT image, (b) results of pre-processing and converting into RGB image, (c) results of segmentation, computed contours of interest objects (CT lung & tumours)

When evaluating, the suppressing noise in addition to the suggested modification of intermediate filters allowed an increase in the delineation of boundaries by 2.2 - 3.9%. A mode of division and visual exemplification of the identified limits of the lungs and nodules is shown in Figure 7. This Figure displays the outcomes of the division and the lung color-coding and the contour detected for objects of interest (lungs & tumours). Table 1 shows the statistics given for the quantification of the detected boundaries and nodules of the lungs on CT images.

Table 1. Statistics of quantitative data on lung boundaries and nodule contours detection

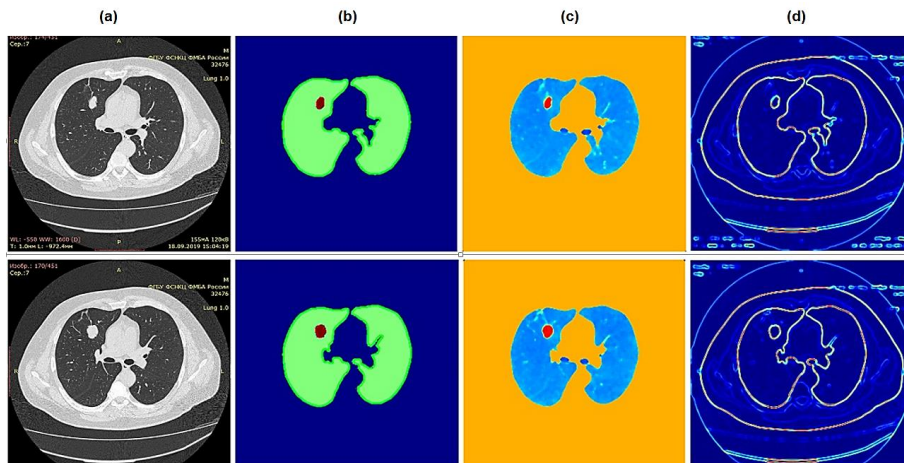| "Estimates"	boundaries of lung				boundaries of Nodules			
	min	*Avg ± SD*	*med*	*max*	*min*	*Avg ± SD*	*med*	*Max*
Ω	0.952	0.969±0.016	0.968	0.985	0.934	0.957±0.033	0.957	0.962
Sen.	0.950	0.985±0.007	0.974	0.996	0.946	0.975±0.012	0.965	0.984
DSC	0.937	0.986 ±0.019	0.970	0.989	0.928	0.959 ±0.021	0.959	0.968
PFM	0.965	0.989±0.011	0.982	0.998	0.945	0.979±0.013	0.963	0.987

Figure 7. Mode of processing: (a) prototype images, (b) segmentation of lung and nodules (to evaluate the characteristic of the lung and tumours as a place of the tumour, size, and form of lung and tumours), (c) color-coded regions to the determination of blood vessels to the tumour, d) color-coded edge map (This helps to identify unknown parts that lead to a tumour in the future)

Based on an expert assessing, we notice the variance in many standards amongst the abilities of the radiologist using a computer program by the techniques of processing a proposed image. Also, it is to be noted that everyone should stick to such criteria because the rate of finding changes that are pathological in addition to data analysis attained leading to processing of the computer to be the winner. Being a part of an empirical study that uses a scanning microscope is to process and analyze data that are observational in the tissue growth and maturation process. To make the comparison for the specificity in evaluating indicators attained utilizing a program on computer considering the suggested methods of processing the estimates of three radiologists with various working experience (15 years, 5 years, and 2 years) were employed. Info regarding the estimates attained is shown in Table 2.

Table 2. Evaluations are performed manually by medical personnel and with the assistance of proposed representations produced by technological technologies

Determined Features	Evaluated by a radiologist	Software performance
Pathology localization	96.1±3.2%	97.8±5.8%
Pathology objects detection	93,4±5.1%	98.7±6.4%
Shape	97,3±1.9%	99.5±4.1%
Size of pathology objects structural elements	0%	99.2±4.5%
Edge	93,1±2%	98.6±2.8%
Relation to other structures	100%	0%
Sensitivity	97,2%	100%

The implant structure filling with elements of the cell was noticed and determined. Such data regarding electron scanning microscopy are indicated by monochrome images at different scales (more than 100). Attained images relying on investigated parts with various resolutions. Resolution diverges from 500×700 to 5120×3840 pixels. When analyzing images with viral pneumonia, the emphasis was placed on the characteristics of the revealed changes corresponding to each CT pattern: compaction of the lung tissue of the "ground glass" type, consolidation, with reticular changes, as well as the percentage of the lung parenchymal, from the size of which the severity of pathological changes is determined. An example of the analysis and interpretation of an image with signs of COVID-19 based on the developed methodology is indicated in Figure 8. It is noticed that a features of brightness and contrast of an image and a segmentation of a medical experiment of the COVID-19 images help in testing the treatment; it will show the size of the infected area before and after processing.
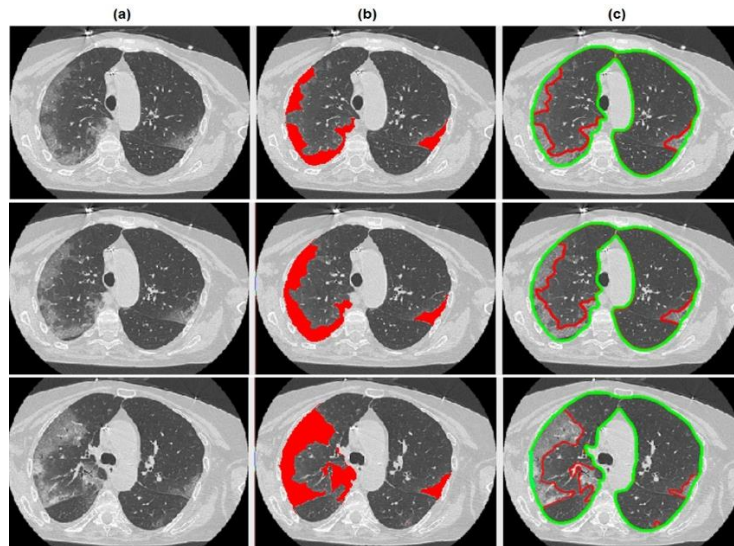
Figure 8. Example of processing CT-COVID-19: (a) original images, (b) segmentation of infected area by the COVID-19 (to evaluate the characteristic of the lung and infected area as a place of the tumour, size, and form of lung and tumours), and (c) edge map of normal and infected areas (green line indicate the real lung and red line indicate to the infected area by the COVID-19)

An example of visual analysis of the developed approach from a patient with confirmed COVID-19 (male, 25 years old) during follow-up from 3 to 14 days of the disease and interpretation of images with markers of COVID-19 shown in Figure 9.
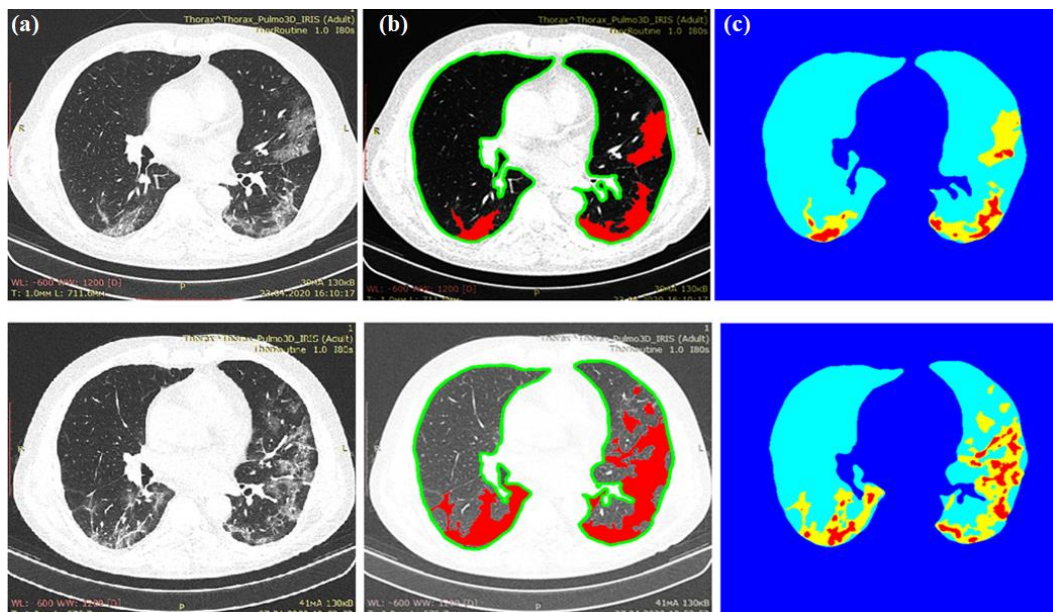

Figure 9. Examples of lung CT processing with COVID-19: (a) the 3rd day of infection with COVID-19, (b) the 14th day of infection with COVID-19, and (c) results of color-map (yellow colour indicates to medium infections, while the red colour indicates to Strong infections (Dangerous Infections))

Figure 9 shows the images on the 3rd and 14th days of infection with COVID-19. One can see a more or less homogeneous tissue of a "crushed glass opacity", the 3rd-day of infection in the right lung with a percentage of 9 % and 4 % on the left with a total infection region of 13, and the 14th-day of infection in the right lung with a percentage of 18 % and 10 % on the left with a total infection region of 28 with an increase in the diameter of blood vessels in the affected area which is characteristic of this disease. The right image shows the proportions of the densest part on both the right and the left in the central regions to the least dense portion along the perimeter, which is 6% to 4% on the 3rd day and 13% to 7%. The development of radionics technology, alongside using modern X-ray equipment, as well as considering a standardized medical assessment protocol,

allows several new quantitative assessments in the image to be obtained, expanding the X-ray diagnostic opinion of a radiologist. A testing study of the analysis of the developed and known methods of (tumours and nodules) is based on the Ω, DSC, and average time using our collected database. The results are presented in Table 3.

Table 3. Comparison of a suggested method with conventional methods (tumours and nodules)

Authors, citation	Ω	DSC	Elapsed time
Xu M. [10]	-	96.71± 0012	846 s.
Zhao J. [17]	93.36	-	-
Dai S. [42]	-	98.58 ± 0016	750 s
Proposed method	96.73	97.64 ± 0021	30 s

Table 2 showing the accuracy of the developed methods by Jaccard similarity index, DSC is 96.73, 97.64, and the average time is 30 seconds, which is more accurate than traditional methods.

The results of quantitative CT COVID-19 images analysis, which are attained using developed methods of computation, are presented in Table 4. Tables show the impact of pre-treatment on the calculated indicators.

Table 4. Statistics of quantitative data on lung boundaries detection and segmentation of infected area by COVID-19 of Figure 7

Patient	The infected area of entire lung %	The normal area of entire lung %	The infected area of left lung %	The infected area of right lung %
Patient 1	5	95	1	4
Patient 2	7	93	2	5
Patient 3	10	90	2	8

A comparative study of the analysis of the developed way and identified methods of (COVID-19) is based on the Ω, DSC, and average time. The outcomes are indicated in Table 5.

Table 5. Comparison of a suggested method with conventional methods (COVID-19)

Authors, citation	DSC %	sensitive
Zhou, T. [11]	69.1	81.1
Fan, D. P. [26]	73.9	72.2
Proposed method	85.3	86.7

The radiologist remarks about the results of the developed method are as follows:

    1. High performance in segmenting infected areas of COVID-19.

    2. Is successful in evaluating infected regions of COVID-19 in right and left lung.

    3. The method may be more advantageous to assess the efficacy of treatment. It can as well help specialists in diagnosis, follow-up, treatment, and isolation of patients.

4. Conclusions

Early CT lung detection plays a vital role in human health. In this paper, a new methodology developed that permits making a system that is automated for lung boundaries, and COVID-19 infection segmentation of CT images, especially to the carcinoma patients, was developed. Image processing techniques were implemented for this segmentation and contours detection task. The inspiration driving the proposed framework is because of the absence of basic and powerful frameworks for fragmenting the lung, tumours, and contaminated areas (COVID-19) on CT images. Broad trials on our COVID-19 dataset, tumours, and knobs have shown that the proposed procedure outflanks the bleeding edge division models and advances the cutting edge exhibitions. The created framework was tried by many influenced and non-influenced images gathered from an online information base. The testing was meant to show the capacity of the proposed framework in separating the little knob contaminated districts by malady COVID-19 on CT images. The proposed methodology for information preparing and representation can speed up a lot of CT images and make it conceivable to recognize little obsessive changes, which additionally lead to an improvement like the radiological end. Our framework can

possibly be applied in surveying the conclusion of COVID-19, e.g., evaluating the contaminated districts, checking the longitudinal illness changes, and mass screening preparing.

References

[1] Z. Ye, Y. Zhang, Y. Wang, Z. Huang, and B. J. E. r. Song, "Chest CT manifestations of new coronavirus disease 2019 (COVID-19): a pictorial review," vol. 30, no. 8, pp. 4381-4389, 2020.

[2] A. S. Abdalrada, O. H. Yahya, A. H. M. Alaidi, N. A. Hussein, H. T. Alrikabi, and T. Al-Quraishi, "A predictive model for liver disease progression based on logistic regression algorithm," *Periodicals of Engineering and Natural Sciences,* Article vol. 7, no. 3, pp. 1255-1264, 2019.

[3] W. H. Organization, "Considerations for quarantine of individuals in the context of containment for coronavirus disease (COVID-19): interim guidance, 19 March 2020," World Health Organization2020.

[4] K. Marhold and J. Fell, "Format Wars Hampering Crisis Response–The Case of Contact Tracing Apps During COVID-19," Available at SSRN, 2020.

[5] W. Zhang, B. Mao, X. Chen, L. Wang, S. Fan, Y. Teng, and Y. Kang, "Low-Dose Computed Tomography Image Denoising with Variance-Stabilizing Transformation and Noise Variance Estimation," Journal of Medical Imaging and Health Informatics, vol. 6, no. 5, pp. 1345-1359, 2016.

[6] R. A. Smith, A. C. von Eschenbach, R. Wender, B. Levin, T. Byers, D. Rothenberger, D. Brooks, W. Creasman, C. Cohen, and C. Runowicz, "American Cancer Society guidelines for the early detection of cancer: update of early detection guidelines for prostate, colorectal, and endometrial cancers: Also: update 2001—testing for early lung cancer detection," vol. 51, no. 1, pp. 38-75, 2001.

[7] M. Al-dabag, H. S. ALRikabi, and R. Al-Nima, "Anticipating Atrial Fibrillation Signal Using Efficient Algorithm," *International Journal of Online and Biomedical Engineering (iJOE),* vol. 17, no. 2, pp. 106-120, 2021.

[8] A. Ghazi, S. Aljunid, A. Fareed, S. Z. S. Idrus, C. M. Rashidi, A. Al-dawoodi, and A. M. Fakhrudeen, "Performance Analysis of ZCC-Optical-CDMA over SMF for Fiber-To-The-Home Access Network," in *Journal of Physics: Conference Series*, 2020, vol. 1529, no. 2, p. 022013: IOP Publishing.

[9] V. Rajinikanth, N. Dey, A. N. J. Raj, A. E. Hassanien, K. Santosh, and N. Raja, "Harmony-search and otsu based system for coronavirus disease (COVID-19) detection using lung CT scan images," *arXiv preprint arXiv,* 2020.

[10] M. Xu, S. Qi, Y. Yue, Y. Teng, L. Xu, Y. Yao, and W. Qian, "Segmentation of lung parenchyma in CT images using CNN trained with the clustering algorithm generated dataset," *Biomedical engineering online,* vol. 18, no. 1, pp. 1-21, 2019.

[11] T. Zhou, S. Canu, and S. Ruan, "An automatic covid-19 ct segmentation based on u-net with attention mechanism," *arXiv preprint arXiv,*2020.

[12] A. Zotin, Y. Hamad, K. Simonov, M. Kurako, and A. Kents, "Processing of CT Lung Images as a Part of Radiomics," in *International Conference on Intelligent Decision Technologies*, 2020, pp. 243-252: Springer.

[13] G. Coppini, M. Miniati, S. Monti, M. Paterni, R. Favilla, and E. Ferdeghini, "A computer-aided diagnosis approach for emphysema recognition in chest radiography," *Medical engineering & physics,* vol. 35, no. 1, pp. 63-73, 2013.

[14] B. Xu and X. J. P. Meng, "A deep learning algorithm using CT images to screen for Corona Virus Disease (COVID-19).", *Preprint.*

[15] L. Li, L. Qin, Z. Xu, Y. Yin, X. Wang, B. Kong, J. Bai, Y. Lu, Z. Fang, and Q. J. R. Song, "Artificial intelligence distinguishes COVID-19 from community acquired pneumonia on chest CT," *Radiology,*2020.

[16] T. Ai, Z. Yang, H. Hou, C. Zhan, C. Chen, W. Lv, Q. Tao, Z. Sun, and L. J. R. Xia, "Correlation of chest CT and RT-PCR testing for coronavirus disease 2019 (COVID-19) in China: a report of 1014 cases," *Radiology,* vol. 296, no. 2, pp. E32-E40, 2020.

[17] J. Zhao, R. Ma, Y. Qiang, and Z. Cui, "Solitary pulmonary nodule segmentation based on the rolling ball method," *Journal of Computational and Theoretical Nanoscience,* vol. 12, no. 8, pp. 1977-1983, 2015.

[18] A. S. Hussein, R. S. Khairy, S. M. M. Najeeb, and H. ALRikabi, "Credit Card Fraud Detection Using Fuzzy Rough Nearest Neighbor and Sequential Minimal Optimization with Logistic Regression," *International Journal of Interactive Mobile Technologies*. vol. 15, no. 5, 2021.

[19] T. M. Deserno, M. Soiron, J. E. De Oliveira, and A. d. A. Araújo, "Computer-aided diagnostics of screening mammography using content-based image retrieval," in *Medical Imaging 2012: Computer-Aided Diagnosis*, 2012, vol. 8315, p. 831527: International Society for Optics and Photonics.

[20] A. Ghazi, S. Aljunid, S. Z. S. Idrus, C. Rashidi, A. Al-dawoodi, B. A. Mahmood, A. Fareed, M. U. Zaenal, N. H. Qasim, and R. M. Rafeeq, "A Systematic review of Multi-Mode Fiber based on Dimensional Code in Optical-CDMA," in *Journal of Physics: Conference Series*, 2021, vol. 1860, no. 1, p. 012016: IOP Publishing.

[21] M. J. Willemink and P. Noël, "The evolution of image reconstruction for CT—from filtered back projection to artificial intelligence," *European radiology,* vol. 29, no. 5, pp. 2185-2195, 2019.

[22] C. Wang, "Segmentation of multiple structures in chest radiographs using multi-task fully convolutional networks," in *Scandinavian Conference on Image Analysis*, 2017, pp. 282-289: Springer.

[23] N. A. Jasim, H. ALRikabi, "Design and Implementation of Smart City Applications Based on the Internet of Things," International Journal of Interactive Mobile Technologies (iJIM), vol. 15, no. 13, pp. 4-15, 2021.

[24] A. G. M. Al-dawoodi, and M. Mahmuddin, "An empirical study of double-bridge search move on subset feature selection search of bees algorithm," *Journal of Telecommunication, Electronic and Computer Engineering,* vol. 9, no. 2-2, pp. 11-15, 2017.

[25] T. M. A. Amphawan, S. Alshwani, and A. Aldawoodi, "Modal Properties of a Varied High Indexed Large Core 4 Mode Photonic Crystal Fiber." *2018 IEEE 7th International Conference on Photonics (ICP)*. IEEE, 2018.

[26] D.-P. Fan, T. Zhou, G.-P. Ji, Y. Zhou, G. Chen, H. Fu, J. Shen, and L. Shao, "Inf-net: Automatic covid-19 lung infection segmentation from ct images," *IEEE Transactions on Medical Imaging,* vol. 39, no. 8, pp. 2626-2637, 2020.

[27] A. Oulefki, S. Agaian, T. Trongtirakul, and A. Laouar, "Automatic COVID-19 lung infected region segmentation and measurement using CT-scans images," *Pattern recognition,* vol. 114, p. 107747, 2021.

[28] A. Zotin, Y. Hamad, K. Simonov, and M. Kurako, "Lung boundary detection for chest X-ray images classification based on GLCM and probabilistic neural networks," *Procedia Computer Science,* vol. 159, pp. 1439-1448, 2019.

[29] A.. Zotin, "Fast algorithm of image enhancement based on multi-scale Retinex," *Procedia Computer Science,* vol. 131, pp. 6-14, 2018.

[30] N. A. Hussein. H. A. Naman, M. Al-dabag, H. Salim, "Encryption System for Hiding Information Based on Internet of Things," *International Journal of Interactive Mobile Technologies (iJIM),* vol. 15, no. 2, 2021.

[31] H. Maraha, K. A. Ameen, O. A. Mahmood, and A. Al-dawoodi, "DWDM over FSO under the effect of different atmospheric attenuations," *ndonesian Journal of Electrical Engineering and Computer Science,* vol. 18, no. 2, pp. 1089-1095, 2020.

[32] D. Abdul-Rahman Al-Malah, H. Th,and H. A. Mutar, "Cloud Computing and its Impact on Online Education," *IOP Conference Series: Materials Science and Engineering,* vol. 1094, p. 012024, 2021.

[33] Y. A. Hamad, K. Simonov, and M. B. Naeem, "Lung Boundary Detection and Classification in Chest X-Rays Images Based on N,ural Network," in *International Conference on Applied Computing to Support Industry: Innovation and Technology*, 2019, pp. 3-16: Springer.

[34] R. M. Al_airaji, I. A. Aljazaery, S. K. Al_dulaimi, and H. T. Salim, "Generation of high dynamic range for enhancing the panorama environment," *Bulletin of Electrical Engineering and Informatics,* Article vol. 10, no. 1, pp. 138-147, 2021.

[35] M. S. Islam, M. Ahsan Ullah, and J. Prakash Dhar, "An imperceptible & robust digital image watermarking scheme based on DWT, entropy and neural network," *Karbala International Journal of Modern Science,* vol. 5, no. 1, p. 6, 2019.

[36] S. A. Ali and A. T. Hashim, "Wavelet transform based technique for text image localization," *Karbala International Journal of Modern Science,* vol. 2, no. 2, pp. 138-144, 2016.

[37] B. Mohammed, R. Chisab, and H. Alrikabi, "Efficient RTS and CTS Mechanism Which Save Time and System Resources," *international Journal of Interactive Mobile Technologies,* vol. 14, no. 4, pp. 204-211, 2020.

[38] J. Zhao, Y. Zhang, X. He, and P. Xie, "Covid-ct-dataset: a ct scan dataset about covid-19," *arXiv preprint arXiv,* vol. 490, 2020.

[39] A. S. Hussein, R. Khairy, H. Salim, "The Detection of Counterfeit Banknotes Using Ensemble Learning Techniques of AdaBoost and Voting," *International Journal of Intelligent Engineering and Systems,* vol. 14, no. 1, pp. 326-339, 2021.

[40] A. Behura, "The cluster analysis and feature selection: Perspective of machine learning and image processing," *Data Analytics in Bioinformatics: A Machine Learning Perspective,* pp. 249-280, 2021.

[41] L. C. Poon, H. Yang, A. Kapur, N. Melamed, B. Dao, H. Divakar, H. D. McIntyre, A. B. Kihara, D. Ayres-de-Campos, and E. Ferrazzi, "Global interim guidance on coronavirus disease 2019 (COVID-19) during pregnancy and puerperium from FIGO and allied partners: Information for healthcare professionals," *International Journal of Gynecology & Obstetrics,* vol. 149, no. 3, pp. 273-286, 2020.

[42] S. Dai, K. Lu, J. Dong, Y. Zhang, and Y. J. N. Chen, "A novel approach of lung segmentation on chest CT images using graph cuts," *Neurocomputing,* vol. 168, pp. 799-807, 2015.